Solar Energy Materials and Solar Cells 168 (2017) 221–226

Contents lists available at ScienceDirect

Solar Energy Materials and Solar Cells

journal homepage: www.elsevier.com/locate/solmat

Superior performance of V_2O_5 as hole selective contact over other transition metal oxides in silicon heterojunction solar cells

Osbel Almora[a], Luis G. Gerling[b,c], Cristóbal Voz[b], Ramón Alcubilla[b,c], Joaquim Puigdollers[b,c,*], Germà Garcia-Belmonte[a,**]

[a] Institute of Advanced Materials (INAM), Universitat Jaume I, 12006 Castelló, Spain
[b] Electronic Engineering Department, Universitat Politècnica de Catalunya, Jordi Girona 1–3, Barcelona 08034, Spain
[c] Centre de Recerca en Nanoenginyeria (CrNE), Pascual Vila 15, Barcelona 08028, Spain

ARTICLE INFO

Keywords:
Transition metal oxides
Silicon solar cells
Impedance spectroscopy
Passivation
Minority carrier lifetime

ABSTRACT

Transition metal oxides (TMOs) have recently been proved to efficiently serve as hole-selective contacts in crystalline silicon (c-Si) heterojunction solar cells. In the present work, two TMO/c-Si heterojunctions are explored using MoO_3 (reference) and V_2O_5 as an alternative candidate. It has been found that V_2O_5 devices present larger (16% improvement) power conversion efficiency mainly due to their higher open-circuit voltage. While V_2O_5/c-Si devices with textured front surfaces exhibit larger short-circuit currents, it is also observed that flat solar cell architectures allow for passivation of the V_2O_5/n-Si interface, giving significant carrier lifetimes of 200 μs (equivalent to a surface recombination velocity of $S_{eff} \sim 140$ cm s^{-1}) as derived from impedance analysis. As a consequence, a significant open-circuit voltage of 662 mV is achieved. It is found that, at the TMO/c-Si contact, a TMO work function enhancement $\Delta\Phi_{TMO}$ occurs during the heterojunction formation with the consequent dipole layer enlargement $\Delta' = \Delta + \Delta\Phi_{TMO}$. Our results provide new insights into the TMO/c-Si contact energetics, carrier transport across the interface and surface recombination allowing for further understanding of the nature of TMO/c-Si heterojunctions.

1. Introduction

During the last decade, crystalline silicon (c-Si) heterojunction solar cells incorporating thin films of hydrogenated amorphous silicon (a-Si:H) have become the state-of-the-art photovoltaic technology, achieving record efficiencies above 26% [1]. The key for the success of this technology lies on the superior surface passivation provided by very thin layers (< 5 nm) of intrinsic a-Si:H, also allowing for carrier conduction with minimal resistive losses. However, performance limitations caused by the relatively high optical absorption of a-Si:H [2] and the highly recombining n/p doped layers [3] (which act as electron/hole selective contacts) have led to investigate novel heterojunction concepts between c-Si and dopant-free highly-transparent transition metal oxides (TMOs) [4,5].

Originally introduced in organic electronics as electron and hole transport layers, TMOs are large band gap (E_g > 3 eV) semiconductors with a wide variety of work functions ($\Phi_{TMO} \sim 3$–7 eV) and conductivities (from insulating to metallic-like), providing great flexibility when used as electron- or hole-selective contact materials [6]. Additionally, they can be deposited at low temperature (T < 200 °C) or by solution-processing methods [7], increasing the potential for process simplification and cost reduction. Until now, hole-selective MoO_3 has been the study-case TMO material alongside n-type crystalline silicon (n-Si), reaching a power conversion efficiency (*PCE*) of 22.5% in a MoO_3/(i)a-Si:H/n-Si configuration [8], where the intrinsic (i)a-Si:H chemically passivates the silicon surface while MoO_3 provides the hole-selectivity. Also rear MoO_x contacts with partial contact areas have been reported with an efficiency of 20.4% [9]. As an alternative, simpler structures comprising TMOs in direct contact with n-Si have also been proposed, achieving efficiencies between 12.5% and 18.4% [10–12].

The unique behavior of MoO_3 and other similar TMOs (V_2O_5, WO_3) is explained by their electronic configuration and large work function values (Φ_{TMO} > 5.0 eV), which upon Fermi level (E_F) alignment with n-Si ($\Phi_{n\text{-}Si} \sim 4.2$ eV) induces a potential barrier (band bending) [10,13]. This is believed to result in the formation of an inversion (p^+) layer upon n-Si where photogenerated holes are collected and then extracted across the TMO/n-Si interface. Recent reports have also proposed V_2O_5 as an interesting alternative to MoO_3, indicating that larger open-circuit

* Corresponding author at: Electronic Engineering Department, Universitat Politècnica de Catalunya, Jordi Girona 1–3, Barcelona 08034, Spain.
** Corresponding author.
E-mail addresses: joaquim.puigdollers@upc.edu (J. Puigdollers), garciag@uji.es (G. Garcia-Belmonte).

http://dx.doi.org/10.1016/j.solmat.2017.04.042
Received 7 February 2017; Received in revised form 25 April 2017; Accepted 26 April 2017

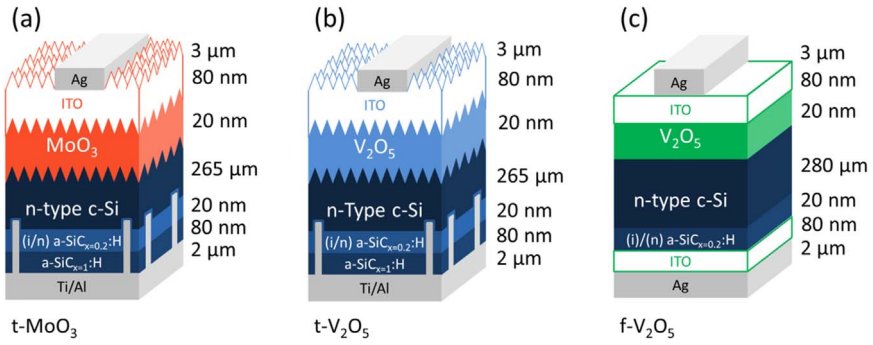

Fig. 1. Sketches of the structures for the three devices which were studied in this work, as indicated.

voltage values (higher hole-selectivity) can be achieved for V_2O_5–based devices with and without the inclusion of passivating (i)a-Si:H interlayers [10–12].

In the present paper, Impedance Spectroscopy (IS) measurements were used to compare the performance of MoO_3 and V_2O_5 as hole-selective contacts in n-Si solar cells, showing that V_2O_5–based solar cells perform better due to higher built-in voltages and enhanced passivation. Additionally, temperature-dependent measurements were used to calculate barrier heights across the interface, giving further details about the energetics of TMO/n-Si heterojunctions.

2. Experimental

2.1. Device fabrication

Solar cells were fabricated with n-type 2 Ω·cm resistivity wafers ($\sim 2.3\times10^{15}$ cm^{-3} dopant concentration) made from float zone monocrystalline (100 orientation) material. The use of such high quality silicon allows for a very high bulk lifetime ($\tau_{bulk}\sim$3 ms under high injection conditions), ensuring almost all recombination paths are confined to the surfaces. Solar cells labeled t-MoO_3 and t-V_2O_5 were subjected to random texturization of the front surface by alkaline etching (~265 µm final wafer thickness), while cells named f-V_2O_5 were processed as purchased (flat polished finish, ~280 µm wafer thickness). After a standard RCA cleaning and 1% HF dip, all substrates were then loaded into a plasma-enhanced chemical vapor deposition (PECVD) system to deposit on the rear side an electron-selective contact consisting of an intrinsic/n-type a-SiC$_x$:H stack (5 nm/15 nm, $x\sim$0.2). Subsequently, two rear contact strategies were used: *1)* t-MoO_3 and t-V_2O_5 cells had an a-SiC$_x$:H back-reflector (80 nm, $x\sim$1) deposited by PECVD which was then laser-fired to obtain an array of locally-diffused point contacts (0.5% contacted area) [14]; *2)* f-V_2O_5 cells had an indium-tin-oxide (ITO) back-reflector/electrode deposited by RF magnetron sputtering (80 nm, 1.3×10^{-3} mbar Ar pressure). As for the front hole-selective contacts, 20 nm thick TMO films were thermally evaporated from powdered V_2O_5/MoO_3 sources (> 99.99% purity, Sigma Aldrich) at $\sim 8\times10^{-6}$ mbar. For the front textured sample, the deposition time was ~1.7 times longer than the polished ones, in order to compensate for the increase in surface area. The deposition rate was ~0.2 Å/s, as controlled by quartz micro-balance, while the substrate remained at room temperature during the process. After a brief air exposure, an ITO front electrode/antireflective layer (80 nm) was also deposited. At this point in the process, quasi-steady state photoconductance (QSSPC) measurements were performed in order to determine the carrier lifetime of the solar cell precursor (Fig. S5). After lithographic patterning of 1 cm^2 active cell areas, a front-contact Ag grid (4.3% shadow losses) was thermally evaporated by use of a shadow mask, while the back-contact metallization was done by e-beam evaporation of Ti/Al (t-MoO_3 and t-V_2O_5) or Ag evaporation (f-V_2O_5).

2.2. Characterizations

The IS measurements at open-circuit voltage V_{oc} (Figs. S7-S9) were carried out using an Autolab PGSTAT-30 potentiostat in the frequency range between 100 mHz and 1 MHz, being the AC perturbation of 10 mV. The spectra were recorded in open-circuit conditions under varying illumination up to 150 mW cm^{-2} (XE 300 W Newport 6258). For achieving this, a bias voltage which corresponds to V_{oc} was applied, hence ensuring a more homogeneous distribution of excess carriers by suppressing DC current. For IS measurements at short-circuit in the dark and at different temperatures (Fig. S3), a Gamry Reference 3000 potentiostat/galvanostat/ZRA (same AC perturbation and frequency range as above) was employed joining the Novocontrol Quatro Cryosystem.

3. Results and discussion

3.1. Device structures and performance

The structure of the three representative devices studied here is presented in the sketches of Fig. 1, including the specifications about composition and thickness of each layer. This set of configurations will allow us to properly compare performances among V_2O_5– and MoO_3–based Si heterojunction solar cells. The first structure, labeled t-MoO_3, uses a 20 nm-thick layer of MoO_3 as front hole-selective contact deposited on a textured surface, while the rear electron-selective contact is formed by a (i/n$^+$)a-SiC$_{x\sim0.2}$:H stack that was locally-diffused by laser firing (Fig. 1a). On the other hand, there are two structures with V_2O_5 as hole selective contact called t-V_2O_5 and f-V_2O_5 (see Fig. 1b and c, respectively). While t-V_2O_5 presents the same structure as t-MoO_3, f-V_2O_5 exhibits a flat superposition of layers, increasing the passivation quality provided by V_2O_5. Moreover, f-V_2O_5 uses indium tin oxide (ITO) as a rear electrode, given that laser firing provides a good ohmic contact at the expense of reduced passivation quality. More details about the devices fabrication and morphological features can be found in previous works [10,15], the experimental section and the Supplementary Information (SI).

Examples of current density-voltage (*J-V*) curves resulting from representative devices measured under illumination are shown in Fig. 2. The corresponding performance parameters such as open-circuit voltage (V_{oc}), short-circuit current (J_{sc}), fill factor (*FF*) and *PCE* are summarized in Table 1. Also histograms in Fig. S1 present the parameter distribution for the complete set of studied samples. In this respect, devices with V_2O_5 show significantly higher *PCE* than those comprising MoO_3 layers. Given that only minor improvements in the photocurrent generation and no clear trend in the *FF* are observed, the superiority of V_2O_5–based solar cells is directly connected to the enhancement in output V_{oc} in comparison with MoO_3. Illustratively, among the samples with surface texturing (t-V_2O_5 and t-MoO_3), t-V_2O_5 has larger J_{sc} while the flat sample (f-V_2O_5) has practically the same J_{sc} as t-MoO_3. Additionally, the V_{oc} differences are apparent with signifi-